ACS APPLIED MATERIALS & INTERFACES

Research Article

www.acsami.org

All-Nanoparticle Self-assembly ZnO/TiO_2 Heterojunction Thin Films with Remarkably Enhanced Photoelectrochemical Activity

Sujun Yuan,[†,§] Jiuke Mu,[†] Ruiyi Mao,[‡] Yaogang Li,[‡] Qinghong Zhang,*[,‡] and Hongzhi Wang*[,†]

[†]State Key Laboratory for Modification of Chemical Fibers and Polymer Materials and [‡]Engineering Research Center of Advanced Glasses Manufacturing Technology, MOE, College of Materials Science and Engineering, Donghua University, Shanghai 201620, P. R. China

[§]School of Materials Science and Engineering, Shanghai University, Shanghai 200444, P. R. China

Supporting Information

ABSTRACT: The multilaminated ZnO/TiO_2 heterojunction films were successfully deposited on conductive substrates including fluorine-doped tin oxide (FTO) glass and flexible indium tin oxide coated poly(ethylene terephthalate) via the layer-by-layer (LBL) self assembly method from the oxide colloids without using any polyelectrolytes. The positively charged ZnO nanoparticles and the negatively charged TiO_2 nanoparticles were directly used as the components in the consecutive deposition process to prepare the heterojunction thin films by varying the thicknesses. Moreover, the crystal growth of both oxides could be efficiently inhibited by the good connection between ZnO and TiO_2 nanoparticles even after calcination at 500 °C, especially for ZnO which was able to keep the crystallite size under 25 nm. The as-prepared films were used as the working electrodes in the three-electrode photoelectrochemical cells. Because the well-contacted nanoscale heterojunctions were formed during the LBL self-assembling process, the ZnO/TiO_2 all-nanoparticle films deposited on both substrates showed remarkably enhanced photoelectrochemical properties compared to that of the well-established TiO_2 LBL thin films with similar thicknesses. The photocurrent response collected from the ZnO/TiO_2 electrode on the FTO glass substrate was about five times higher than that collected from the TiO_2 electrode. Owing to the absence of the insulating layer of dried polyelectrolytes, the ZnO/TiO_2 all-nanoparticle heterojunction films were expected to be used in the photoelectrochemical device before calcination.

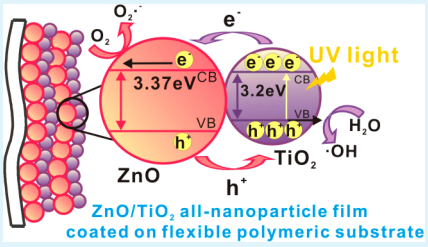

KEYWORDS: *all-nanoparticle, layer-by-layer self-assembly, photoelectrochemical, zinc oxide, titania, heterojunction*

1. INTRODUCTION

Photocatalytic semiconducting materials have been demonstrated to be quite effective in the applications of solar power,[1,2] water treatment,[3−5] and self-cleaning surfaces.[6−9] Among them, TiO_2 and ZnO have been extensively investigated due to their high chemical stability, absence of toxicity, and capability of photooxidative destruction of most organic pollutants. However, the recombination of photogenerated electron/hole pairs always causes a reduction in the photocatalytic efficiency of photocatalysts. In the past years, some methods related to the improvement in photocatalytic activity of TiO_2 or ZnO were reported, such as doping, metal deposition, surface sensitization, and coupling of semiconductors.[10−12] Combining some semiconductors with different band gaps to form heterojunctions is thought to be the most promising technology for increasing the electron/hole pair separation efficiency and extending the energy range of photoexcitation.[13−15] Among the semiconductor couples, the integration of ZnO with TiO_2 is one of the candidates with the biggest concern.[15−18] Contrary to the powder form, ZnO/TiO_2 films have more advantages for practical applications; for instance, they easily connect to an external electrical source and can be recovered and recycled after reactions. Moreover, the ZnO/TiO_2 heterojunction films also have been reported to show much higher photocatalytic and photoelectrocatalytic properties than that of the bare TiO_2 or ZnO films.[19−21] However, in most studies, it was found that the connection of different oxide nanoparticles in the heterojunctions was not ample enough, and the present methods for preparing heterojunction films were not suitable for the flexible polymeric substrates. Therefore, how to obtain the nanoscale heterojunction films with the enhanced performance on flexible polymeric substrates is still a challenge.

Layer-by-layer (LBL) self assembly, as a versatile bottom-up nanofabrication method to prepare multilayered films, is mainly based on the alternate adsorption of oppositely charged species on solid surfaces.[22] The components of the multilayered assemblies in this method usually include polyelectrolytes and inorganic nanoparticles.[23−25] As shown in Figure 1a, to obtain a semiconductive oxide thin film with high activities, the heat post-treatment at a high temperature (usually at 500 °C) is necessary to remove the insulating polyelectrolytes. However, some of the polyelectrolytes still remain after calcination, which causes a detrimental effect on the performance of the films.

Received: January 15, 2014
Accepted: March 26, 2014
Published: March 26, 2014

   dx.doi.org/10.1021/am500314n | ACS Appl. Mater. Interfaces 2014, 6, 5719−5725

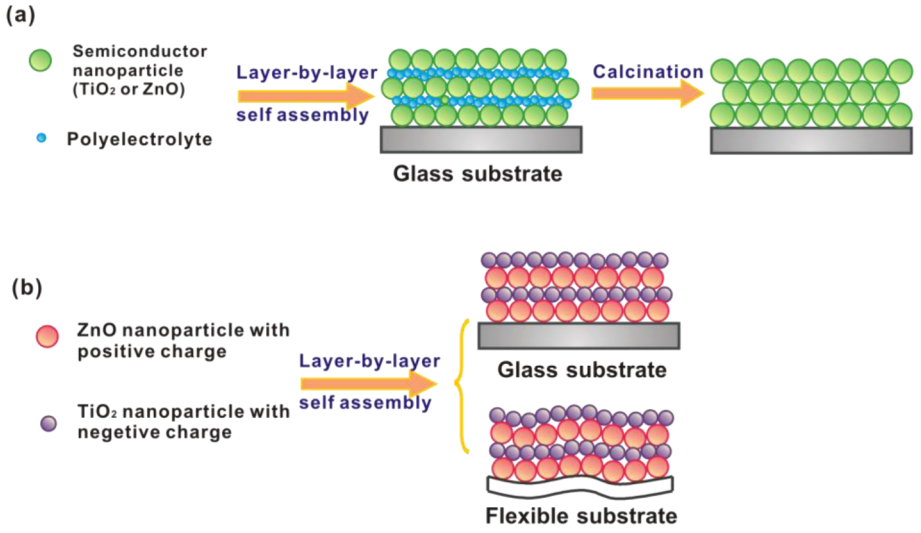

Figure 1. Schematic diagrams of (a) the traditional process for preparing the LBL thin films and (b) the process for preparing the all-nanoparticle ZnO/TiO_2 films.

Kumar and coworkers prepared nanocrystalline TiO_2 electrodes for dye-sensitized solar cell through the LBL self assembly technique. After calcination, it was observed that the more residual polyelectrolyte inside the final TiO_2 electrodes, the poorer the performance of the cell.[26] These problems may be solved if the polyelectrolytes can be replaced by some oppositely charged inorganic nanoparticles, and this all-nanoparticle self-assembly was pioneered by Rubner and coworkers.[27] It also evidently shows the interest in low-temperature ways to fabricate crystalline thin films, since the polyelectrolytes are not used and calcination is avoided. The all-nanoparticle self-assembly nanoparticles are allowed to be deposited on low thermally resistant material substrates, particularly the one with flexible polymeric transparent conductive oxide (as shown in Figure 1b). Meanwhile, the production yield of the film thickness will be doubled compared to that obtained in conventional LBL self assembling. The LBL thin films derived from oppositely charged semiconductor nanoparticles without any polyelectrolytes have not been well known except Rubner's pioneering reports about the all-nanoparticle-based coatings via the layer-by-layer deposition of semiconducting TiO_2 and insulating SiO_2 nanoparticles.[27−29] The obtained TiO_2/SiO_2 films exhibited good antireflectance, antifogging (superhydrophilicity), and self-cleaning properties, but SiO_2 is insulating, which limits the application of the films in semiconductor device fields, especially in photoelectrochemistry. In this work, the heterojunction films through the layer-by-layer self assembling of the positively charged ZnO nanoparticles and the negatively charged TiO_2 nanoparticles were successfully deposited both on fluorine-doped tin oxide (FTO) conductive glass substrates and on indium tin oxide coated poly(ethylene terephthalate) (ITO-PET) conductive film substrates at room temperature. The photoelectrochemical property of the ZnO/TiO_2 films was remarkably enhanced due to the well-connected nanoscale heterostructure.

2. EXPERIMENTAL SECTION

2.1. Preparation of ZnO Sol and TiO_2 Sol. The ZnO sol was prepared using same route as follows.[30] A 0.025 mol portion of $Zn(CH_3OO)_2{\cdot}2H_2O$ was put into a reflux apparatus filled with 300 mL anhydrous ethanol and kept at 80 °C until a transparent solution I was obtained. A 0.024 mol portion of $LiOH{\cdot}H_2O$ was dissolved in 200 mL anhydrous ethanol to get solution II. The key procedure was to make solution II drop into solution I slowly, and then, sonicate the mixture for about 1 h to get the ZnO sol.

TiO_2 sol was obtained from titanium(IV) bis(ammonium lactate) dihydroxide (TALH, 50 wt % in H_2O, Aldrich) through a homogeneous hydrolysis and subsequently hydrothermal process. A 12.2 mL portion of TALH was diluted in 400 mL of the distilled water, and then, 13.8 g urea was added and vigorously stirred for 1 h under room temperature. The mixture was subjected to oil bath at 95 °C for 24 h under magnetic stirring and reflux. After cooling to room temperature, a gel-like precipitate was collected by centrifugation and washed twice with distilled water. The well-washed gel was dispersed in distilled water at a concentration of 10 $g{\cdot}L^{-1}$ and sealed in a Teflon-lined autoclave (80 mL capacity) at 150 °C for a duration of 24 h to improve the crystallinity of the TiO_2 nanoparticles.

Both the ZnO sol and the TiO_2 sol were obtained under mild conditions, and the pH values of these two colloids were close to 7. Therefore, in this work, the ZnO nanoparticles (the isoelectric point is about pH = 9) were positively charged;[31,32] whereas the anatase TiO_2 nanoparticles (the isoelectric point is about pH = 6) were negatively charged.[33,34]

2.2. Preparation of ZnO/TiO_2 Multilayered Films. The as-prepared ZnO with positive charges and TiO_2 with negative charges were used to fabricate the all-nanoparticle multilayered films, which were deposited onto fluorine-doped tin oxide conductive glass substrates (14 $\Omega{\cdot}\square^{-1}$, Nippon Sheet Glass, Hyogo, Japan) and indium tin oxide coated poly(ethylene terephthalate) substrates (20 $\Omega{\cdot}\square^{-1}$, Solutia, St. Louis, Missouri, USA) via the layer-by-layer self assembly technique. It could be produced through the following process; both FTO glasses and ITO-PET substrates were ultrasonically cleaned in water and ethanol for 10 min each. The cleaned substrates were immersed alternately for 15 min in a 0.05 wt % diluting ZnO sol and in a 0.045 wt % diluting TiO_2 sol. After each immersion, the films were washed by distilled water for 60 s. This procedure was repeated for the desired number of cycles to form ZnO/TiO_2 multilayered films.

2.3. Characterization. Some of the ZnO sol and TiO_2 sol were dried at 60 °C and ground into a fine powder for further characterization. The X-ray diffraction (XRD) patterns of these two dried sol powder phase compositions and the ZnO/TiO_2 heterojunction films were identified by X-ray diffractometer (Model D/Max-2550, Rigaku, Tokyo, Japan) using Cu Kα radiation (λ = 1.5406 Å) at 60 kV and 450 mA and that of the films was obtained with an incident angle of 1°. The morphologies of the ZnO and TiO_2 nanoparticles in colloids and films were observed by transmission electron microscopy (TEM; Model JEM-2100F, JEOL, Tokyo, Japan). The structural and

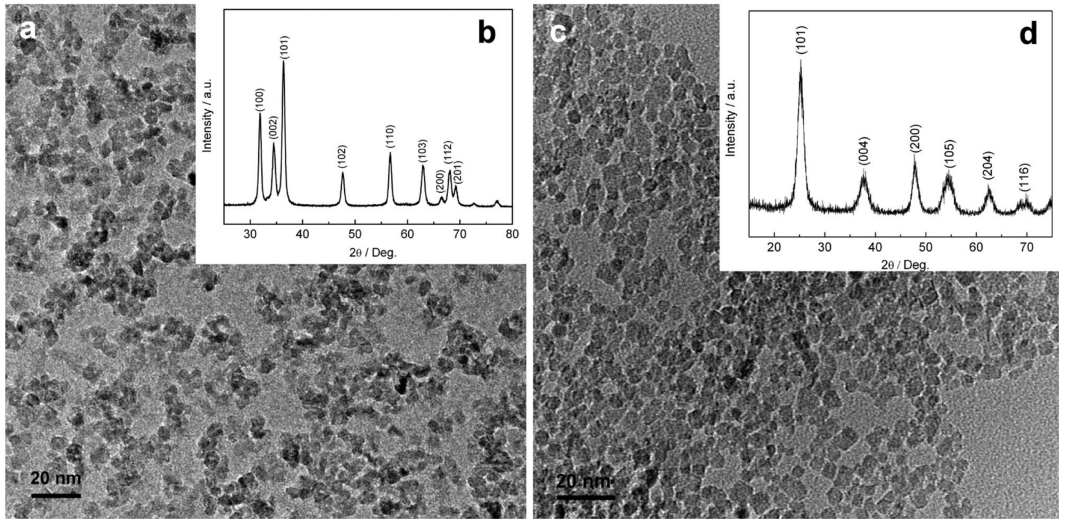

Figure 2. Morphologies and XRD patterns of the nanoparticles used in the layer-by-layer self assembly process: (a and b) ZnO; (c and d) TiO_2.

morphological profiles of the all-nanoparticle multilayered films were carried out by atomic force microscopy (AFM, NanoScope IV, Veeco Instrument, USA) and field-emission scanning electron microscopy (FESEM, Model S-4800, Hitachi, Tokyo, Japan). The UV-vis absorption spectra of the ZnO/TiO_2 multilayered films was recorded by the spectrophotometer (Model Lambda 950, Perkin Elmer, USA), and their thicknesses were measured with the surface profilometer (Wyko NT9100, Veeco Instrument, USA).

2.4. Photoelectrochemical Measurements. The photoelectrochemical properties of the all-nanoparticle multilayered films were studied in three-electrode photoelectrochemical bulk cells at room temperature (25 °C). The films deposited on various substrates with ca. 1.2 cm^2 were used as working electrodes. The width and length of the electrode were 20 and 6 mm, respectively. The reference and counter electrodes were served by a saturated Ag/AgCl electrode and a platinum wire, respectively. The bending test was carried out by a lab-developed flexible electrode bending tester,[35] and the bending radius was adjusted to 10, 12, and 14 mm, respectively (see Figure S1a in the Supporting Information). The measurements of photocurrent responses and electrochemical impedance spectroscopy (EIS) in this study were carried out through an electrochemical workstation (Zennium, ZAHNER-Elektrik, Germany) coupled with a computer. Illumination was carried out using a 4 W UV lamp (F4T5, Bolitong Lumination, Shanghai, China) with the intensity of 1.2 $mW{\cdot}cm^{-2}$, which was measured at 365 nm wavelength by a UV irradiance meter (UV-A, Instruments of Beijing Normal University, China) at the electrode surface. The EIS was measured at zero anodic bias, and the frequency was changed from 100 kHz to 0.1 Hz.

3. RESULTS AND DISCUSSION

3.1. Phase Characterization and Morphologies of the ZnO Sol and TiO_2 Sol. Due to the poor stability of ZnO in water, the ZnO colloid was synthesized according to the procedure reported by Spanhel and Anderson;[36] the as-obtained colloid was well dispersed in ethanol and was suitable for the preparation of the LBL films. Figure 2a shows the TEM micrograph of the ZnO sol, and the inset is the corresponding XRD pattern. According to the XRD result, the diffraction peaks coincide exactly with the JCPDS data of ZnO crystallizing in the hexagonal wurtzite structure, which implies that the ZnO nanoparticles in the sol were well crystallized by refluxing at 80 °C. From the TEM image, the well dispersed nanoparticles of the ZnO sol present a narrow size distribution of 8−12 nm.

The as-prepared TiO_2 colloidal solution could be kept at room temperature in closed vessels for several months without any stabilizer. Therefore, the TiO_2 nanoparticles were used as starting building blocks with the negative charges in the all-nanoparticle films preparation. The TEM image and XRD pattern of the TiO_2 colloidal particles are given in Figure 2b. From the XRD result, it is affirmed that the TiO_2 nanoparticles of the colloid are in the anatase phase. As shown in the TEM micrograph, the TiO_2 nanocrystals are almost in a uniform size with a highly dispersible ability, and the average size of them estimated from the TEM image is ca. 7 nm, which is in good agreement with the value calculated from the (101) diffraction peak of the XRD pattern by using the Scherrer equation (7.4 nm).

3.2. Morphologies of ZnO/TiO_2 Thin Films. The surface morphologies of the eight-bilayered ZnO/TiO_2 LBL films both on the FTO glass substrate and the PET-ITO substrate were characterized by field-emission scanning electron microscopy and tapping mode atomic force microscopy. For comparison, the surface images of the FTO glass and the PET-ITO substrate are shown as well. Very similar FESEM images are observed for multilayered all-nanoparticle films on these two substrates, which are shown in Figure 3b and d, respectively. The surface of the films is composed of tiny grains. No obvious void is observed among the grains, and the roughness of the surface is estimated to be not much greater than the size of the individual nanoparticles. This is consistent with the results using the AFM technique to characterize these films shown in Figure 4. The values of smoothing surface roughness of the films on the two substrates are close—9.9 and 10.6 nm, respectively—indicating their similar roughness and surface areas. All these results demonstrated that the all-nanoparticle thin films with a quite fine structure were successfully deposited on these two substrates and the structure of the films coated on the flexible substrate was as stabile as that of the films coated on the glass substrate.

3.3. Optical Properties of ZnO/TiO_2 Thin Films. The UV−vis absorption spectra of the bare quartz slide and the ones deposited with different layers of ZnO/TiO_2 LBL films are shown in Figure 5. All the self-assembled thin films were proved to have uniform deposition by the UV−vis measurement. The results show a small absorption band edge shift for the as-

dx.doi.org/10.1021/am500314n | ACS Appl. Mater. Interfaces 2014, 6, 5719−5725

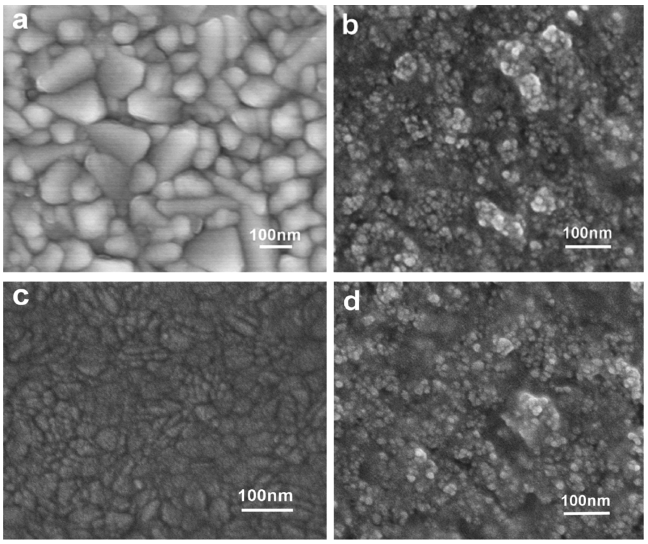

Figure 3. FESEM micrographs of (a) bare FTO glass, (c) bare ITO-PET substrate, and the eight-bilayered ZnO/TiO_2 LBL thin films coated on the (b) FTO glass substrate and (d) ITO-PET substrate.

prepared ZnO/TiO_2 films to 380 nm (3.27 eV) in comparison to that for bulk ZnO (3.37 eV)[37] and anatase TiO_2 (3.2 eV).[38] Moreover, an obvious increase in absorbance at ca. 360 nm can be seen as the layer number increasing, which agrees with the results of the film-thickness obtained from the surface profilometer (the thicknesses of ZnO/TiO_2 thin films were 52.1, 107.2, and 153.8 nm, respectively). The average deposition thickness of each self assembling cycle was ca. 13.1 nm. Layer-by-layer self assembly technique is always applied to obtain the films through the electrostatic interactions, and the adsorbing amount of semiconductor nanoparticles is close to the same in each deposition cycle.[39] Thus, the almost linear increase in film thickness following an increase in layer numbers is explained, and it is also implied that the all-nanoparticle ZnO/TiO_2 films had a fine and quite homogeneous structure.

3.4. Photoelectrochemical Properties of ZnO/TiO_2 Heterojunction Films. To investigate the photoelectrochemical properties of the all-nanoparticle ZnO/TiO_2 films, the transient photocurrent responses of the ZnO/TiO_2 LBL film electrodes both on FTO glass and on ITO-PET in seven on–off cycles of UV light irradiation are given in Figure 6, which were performed in 1 mM $NaNO_3$ solution at +0.4 V vs. Ag/AgCl. As shown in Figure 6, the dark current is approximately zero for all the electrodes, which suggests that no electrochemical oxidization occurred without UV illumination. In contrast, all the apparent photoresponses of the electrodes are obtained after switching on the UV light and then reach a steady state. The photocurrent extent of an electrode can be considered as its photocatalytic oxidation capacity. Higher responsive photocurrent response implies higher oxidation efficiency. In this work, the photocurrents obtained from the

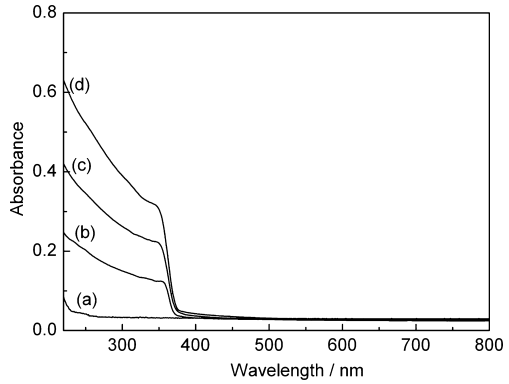

Figure 5. UV–vis absorption spectra of the ZnO/TiO_2 LBL films on quartz slides with different bilayers: (a) bare quartz slide, (b) 4 bilayers, (c) 8 bilayers, and (d) 12 bilayers.

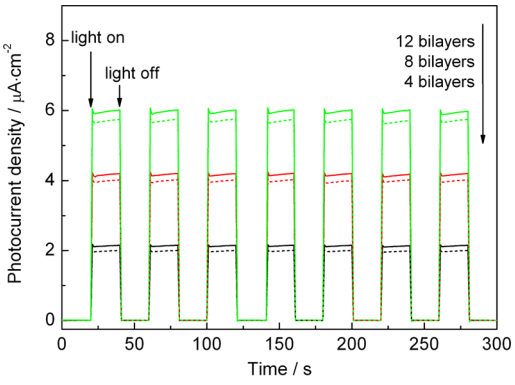

Figure 6. Photocurrent density–time curves of ZnO/TiO_2 LBL thin film electrodes both on glass FTO substrates (solid line) and ITO-PET substrates (dash line) towards 1 mM $NaNO_3$ aqueous solution under UV light irradiation. Applied potential: +0.4 V vs Ag/AgCl. Light intensity: 1.2 $mW \cdot cm^{-2}$.

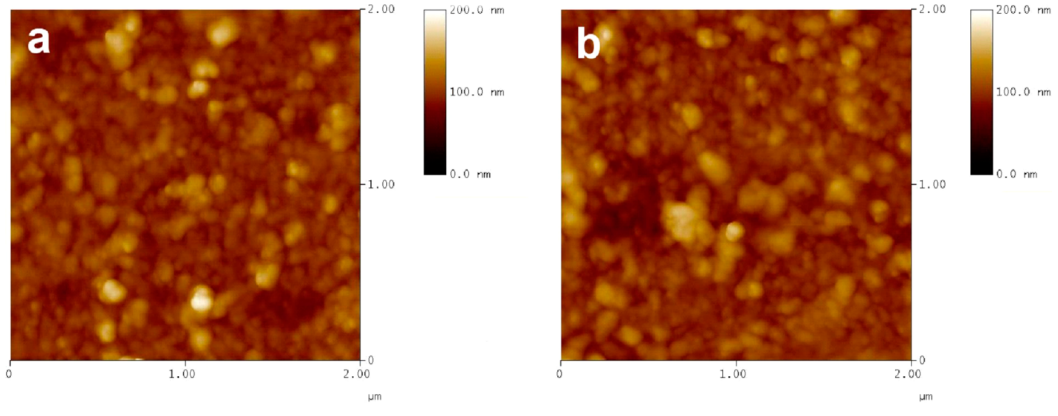

Figure 4. AFM images of the eight-bilayered ZnO/TiO_2 LBL thin film coated on the FTO glass substrate (a) and on the ITO-PET substrate (b).

dx.doi.org/10.1021/am500314n | ACS Appl. Mater. Interfaces 2014, 6, 5719–5725

electrodes on these two substrates rose with the increasing layers of the films and both 12-bilayered ZnO/TiO_2 LBL film electrodes showed enhanced photocurrent responses.

In addition, the photoelectrochemical properties of the ZnO/TiO_2 LBL film electrodes on ITO-PET under bending state were also investigated. Figure S1b in the Supporting Information shows the transient photocurrent responses of the flexible eight-bilayered ZnO/TiO_2 film electrode measured under the bending state with various bending radii. In Figure S1b, it can be found that the photocurrent densities decrease by reducing the bending radius. However, when the bending radius is larger than 12 mm, the photocurrent responses are not significantly influenced, indicating the fair mechanical stability of the ZnO/TiO_2 films prepared by the layer-by-layer self assembly. Due to the remarkably enhanced efficiency as well as the substrates ranged from the polymer to glass, ZnO/TiO_2 films derived from the room-temperature all-nanoparticle LBL self assembly is expected to be applied to both chemical sensors and dye-sensitized solar cells.

3.5. Heterojunction Structure of the All-Nanoparticle ZnO/TiO_2 Films. To further study the heterojunction structure of the ZnO/TiO_2 LBL films, the eight-bilayered all-nanoparticle film electrode coated on FTO glass substrate was calcined at 500 °C for 4 h. Figure 7 presents the morphologies and XRD pattern of the calcined eight-bilayered ZnO/TiO_2 LBL films. As shown in Figure 7a, ZnO/TiO_2 nanoparticles formed a dense film after calcination, and a partial coarsening occurred during the heating treatment. However, the crystallite size of both oxides did not increase apparently. It is found in the TEM images that the crystalline size of the ZnO/TiO_2 LBL films is in the range of 10−25 nm, and the TiO_2 and ZnO nanoparticles tightly contacted with each other (shown in Figure 7b). From the corresponding high-resolution TEM image of the films shown in the inset in Figure 7b, the clear and identical crystallographic orientations of the TiO_2 and ZnO can be observed. The lattice fringes of 0.35 and 0.26 nm concur well with interplanar spacing of (101) and (002) crystallographic planes of anatase TiO_2 and hexagonal ZnO, respectively. In our previous work, it was demonstrated that the growth of ZnO nanoparticles was very remarkable in the absence of flaky layered double hydroxides, and the as-prepared bare ZnO nanoparticles in a crystallite size of 15.0 nm grew to 74.7 nm after calcination at 500 °C.[40] As shown in the inset in Figure 7b, TiO_2 has a crystallite size of 8 nm while ZnO has a crystallite size of 11 nm. In this study, due to the laminated layer-by-layer film structure, the further growth of both ZnO and TiO_2 nanocrystals was inhibited during the heat treatment since the mass transport was hindered by the another oxide composition. The result of the XRD pattern shown in the inset in Figure 7a also supports it. The broadened diffraction peaks of hexagonal ZnO and anatase TiO_2 can be observed in the XRD pattern of the ZnO/TiO_2 LBL films coated on FTO glass which was collected at an incident angle of 1°. The intense diffraction peaks at 31.6°, 34.3°, 36.1°, and 56.3° correspond to the (100), (002), (101), and (110) planes of ZnO, and the ones at 48.1° and 53.8° are assigned to the (200) and (105) planes of anatase TiO_2. All the results implied that the ZnO and TiO_2 nanoparticles kept a good connection during the layer-by-layer self assembling process, which ensured that the all-nanoparticle films were in a good heterojunction structure.

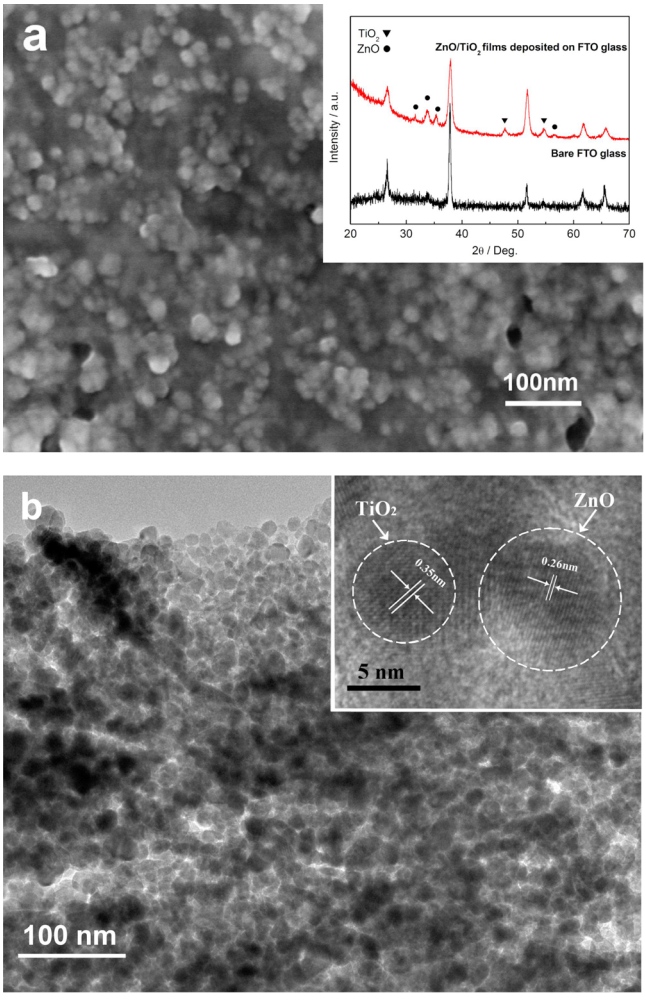

Figure 7. (a) FESEM micrograph and XRD pattern and (b) TEM images of the eight-bilayered ZnO/TiO_2 LBL films on FTO glass substrate after calcination.

The transient photocurrent responses and the Nyquist plots of the calcined eight-bilayered ZnO/TiO_2 LBL film and the calcined TiO_2 LBL film deposited on FTO glass substrates are shown in Figure 8. TiO_2 LBL film in a thickness as similar as that of eight-bilayered ZnO/TiO_2 film, was prepared via the well-established LBL self assembly from an aqueous anatase TiO_2 sol and the poly(styrene sulfonic acid) sodium solution.[41] In Figure 8a, the photocurrent response of the ZnO/TiO_2 film electrode is about five times higher than that of the TiO_2 film electrode. The photocurrent result indicated that the remarkably enhanced photocatalytic performance of all-nanoparticle film could be ascribed to the coupling of ZnO and TiO_2 nanocrystallites to form the heterojunction structure, which achieved a more efficient charge separation, an increased lifetime of the charge carriers, and an enhanced interfacial charge transfer to adsorbed substrates.[42] Moreover, it is noticed that the photocurrent response of the eight-bilayered ZnO/TiO_2 film electrode on the ITO-PET substrate is also high: it is about four times higher than that of the TiO_2 film electrode. This fact suggested that the well-contacted nanoscale heterojunctions had formed during the layer-by-layer self assembling process and implied that the heat treatment was not a necessary step in preparation of the all-nanoparticle LBL films. On the other hand, in order to reveal the interfacial characteristics of the ZnO/TiO_2 heterojunction film electrode, the electrochemical impedance spectroscopy (EIS) spectra of these two samples were studied by applying a small ac

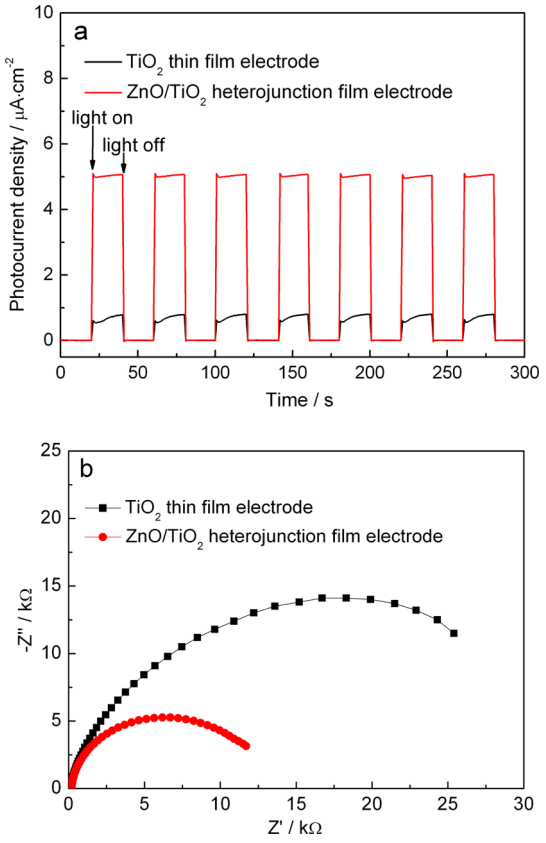

Figure 8. (a) Photocurrent density−time curves and (b) Nyquist plots of the eight-bilayered ZnO/TiO_2 LBL thin film electrode and the TiO_2 LBL film electrode on FTO glass substrates after calcination towards 1 mM $NaNO_3$ aqueous solution under UV light irradiation.

perturbation (10 mv) under UV illumination. Figure 8b shows the Nyquist plots of these two calcined LBL thin film electrodes. Both plots display a single semicircle at the high-frequency region which indicates the charge transfer process.[43] In Figure 8b, it is found that the charge transfer resistance of the ZnO/TiO_2 film electrode is smaller than that of TiO_2 film electrode, which is consistent with the result of the photocatalytic performance. According to the work reported by Boschloo et al.,[44] ZnO nanocrystals had the reduced recombination rate compared to that of TiO_2, thus ZnO/TiO_2 heterojunction films composed from the series connection of TiO_2 with a better electron transport material ZnO were favorable for the electron transfer at the interface and for the charge separation.[45]

CONCLUSIONS

The positively charged ZnO nanoparticles and the negatively charged TiO_2 nanoparticles were used as the components to prepare well-contacted nanoscale heterojunctions through the layer-by-layer self assembly technique. The all-nanoparticle films were directly deposited on the flexible transparent conductive oxide substrates since no polyelectrolyte was used in the self assembling process and the heat treatment was avoided. The photoelectrochemical properties of the films were investigated in three-electrode photoelectrochemical cells. Due to the well-connected heterojunction structure, the improved separation efficiency of photoexcited charge carriers was achieved and the photocurrent densities of the ZnO/TiO_2 thin films on the FTO glass substrate showed a five times enhanced intensity compared to that of the TiO_2 LBL film with similar thickness. This study demonstrated that the all-nanoparticle layer-by-layer self assembly technique could provide a novel and efficient way to prepare heterojunction films. By this route, the all-nanoparticle films from different semiconductors of functional nanoparticles are expected to be fabricated, and they may exhibit remarkably enhanced performance due to the good connection within nanoscale heterojunctions.

ASSOCIATED CONTENT

Supporting Information

Schematic of the bending test and photocurrent density−time curves of electrodes on flexible ITO-PET after bending. This material is available free of charge via the Internet at http://pubs.acs.org.

AUTHOR INFORMATION

Corresponding Authors

*Tel: +86-21-67792943. Fax: +86-21-67792855. E-mail address: zhangqh@dhu.edu.cn (Q.Z.).
*E-mail: wanghz@dhu.edu.cn (H.W.).

Notes

The authors declare no competing financial interest.

ACKNOWLEDGMENTS

We gratefully acknowledge the financial support by the National Key Technology R&D Program (2013BAE01B03), Specialized Research Fund for the Doctoral Program of Higher Education (20110075130001), Science and Technology Commission of Shanghai Municipality (12 nm0503900,13JC1400200), the Program for Professor of Special Appointment (Eastern Scholar) at Shanghai Institutions of Higher Learning, Innovative Research Team in University (IRT1221) and the Program of Introducing Talents of Discipline to Universities (No.111-2-04), and China Postdoctoral Science Foundation funded project (2013M540353).

REFERENCES

(1) Grätzel, M. Photoelectrochemical Cells. *Nature* **2001**, *414*, 338−344.
(2) Frank, A. J.; Kopidakis, N.; van de Lagemaat, J. Electrons in Nanostructured TiO_2 Solar Cells: Transport, Recombination and Photovoltaic Properties. *Coord. Chem. Rev.* **2004**, *248*, 1165−1179.
(3) Zhang, Q. H.; Fan, W. G.; Gao, L. Anatase TiO_2 Nanoparticles Immobilized on ZnO Tetrapods as a Highly Efficient and Easily Recyclable Photocatalyst. *Appl. Catal., B* **2007**, *76*, 168−173.
(4) Kandavelu, V.; Kastien, H.; Thampi, K. R. Photocatalytic Degradation of Isothiazolin-3-ones in Water and Emulsion Paints Containing Nanocrystalline TiO_2 and ZnO Catalysts. *Appl. Catal., B* **2004**, *48*, 101−111.
(5) Wu, J. J.; Tseng, C. H. Photocatalytic Properties of nc-Au/ZnO Nanorod Composites. *Appl. Catal., B* **2006**, *66*, 51−57.
(6) Shi, F.; Wang, Z.; Zhang, X. Combining a Layer-by-Layer Assembling Technique with Electrochemical Deposition of Gold Aggregates to Mimic the Legs of Water Striders. *Adv. Mater.* **2005**, *17*, 1005−1009.
(7) Wu, D.; Wu, S. Z.; Chen, Q. D.; Zhang, Y. L.; Yao, J.; Yao, X.; Niu, L. G.; Wang, J. N.; Jiang, L.; Sun, H. B. Curvature-Driven Reversible In Situ Switching Between Pinned and Roll-Down Superhydrophobic States for Water Droplet Transportation. *Adv. Mater.* **2011**, *23*, 545−549.
(8) Lai, Y. K.; Tang, Y. X.; Gong, J. J.; Gong, D. G.; Chi, L. F.; Lin, C. J.; Chen, Z. Transparent Superhydrophobic/Superhydrophilic TiO_2-

Based Coatings for Self-Cleaning and Anti-Fogging. *J. Mater. Chem.* **2012**, *22*, 7420−7426.
(9) Anandan, S.; Rao, T. N.; Sathish, M.; Rangappa, D.; Honma, I.; Miyauchi, M. Superhydrophilic Graphene-Loaded TiO_2 Thin Film for Self-Cleaning Applications. *ACS Appl. Mater. Interfaces* **2013**, *5*, 207−212.
(10) Szabó-Bárdos, E.; Czili, H.; Horváth, A. Photocatalytic Oxidation of Oxalic Acid Enhanced by Silver Deposition on a TiO_2 Surface. *J. Photochem. Photobiol., A* **2003**, *154*, 195−201.
(11) Yang, G. D.; Yan, Z. F.; Xiao, T. C. Low-Temperature Solvothermal Synthesis of Visible-Light-Responsive S-Doped TiO_2 Nanocrystal. *Appl. Surf. Sci.* **2012**, *258*, 4016−4022.
(12) Han, F.; Kambala, V. S. R.; Srinivasan, M.; Rajarathnam, D.; Naidu, R. Tailored Titanium Dioxide Photocatalysts for the Degradation of Organic Dyes in Wastewater Treatment: A Review. *Appl. Catal., A* **2009**, *359*, 25−40.
(13) Wang, C.; Zhao, J. C.; Wang, X. M.; Mai, B. X.; Sheng, G. Y.; Peng, P. A.; Fu, J. M. Preparation, Characterization and Photocatalytic Activity of Nano-Sized ZnO/SnO_2 Coupled Photocatalysts. *Appl. Catal., B* **2002**, *39*, 269−279.
(14) Yang, G. D.; Yan, Z. F.; Xiao, T. C. Preparation and Characterization of SnO_2/ZnO/TiO_2 Composite Semiconductor With Enhanced Photocatalytic Activity. *Appl. Surf. Sci.* **2012**, *258*, 8704−8712.
(15) Wang, C.; Xu, B. Q.; Wang, X. M.; Zhao, J. C. Preparation and Photocatalytic Activity of ZnO/TiO_2/SnO_2 Mixture. *J. Solid State Chem.* **2005**, *178*, 3500−3506.
(16) Lin, L.; Yang, Y. C.; Men, L.; Wang, X.; He, D. N.; Chai, Y. C.; Zhao, B.; Ghoshroy, S.; Tang, Q. W. A Highly Efficient TiO_2@ZnO n−p−n Heterojunction Nanorod Photocatalyst. *Nanoscale* **2013**, *5*, 588−593.
(17) He, Z. Y.; Li, Y. G.; Zhang, Q. H.; Wang, H. Z. Capillary Microchannel-Based Microreactors with Highly Durable ZnO/TiO_2 Nanorod Arrays for Rapid, High Efficiency and Continuous-Flow Photocatalysis. *Appl. Catal., B* **2010**, *93*, 376−382.
(18) Athauda, T. J.; Neff, J. G.; Sutherlin, L.; Butt, U.; Ozer, R. R. Systematic Study of the Structure−Property Relationships of Branched Hierarchical TiO_2/ZnO Nanostructures. *ACS Appl. Mater. Interfaces* **2012**, *4*, 6917−6926.
(19) Marcì, G.; Augugliaro, V.; López-Muñoz, M. J.; Martín, C.; Palmisano, L.; Rives, V.; Schiavello, M.; Tilley, R. J. D.; Venezia, A. M. Preparation Characterization and Photocatalytic Activity of Polycrystalline ZnO/TiO_2 Systems. 2. Surface, Bulk Characterization, and 4-Nitrophenol Photodegradation in Liquid−Solid Regime. *J. Phys. Chem. B* **2001**, *105*, 1033−1040.
(20) Kim, D. W.; Lee, S.; Jung, H. S.; Kim, J. Y.; Shin, H.; Hong, K. S. Effects of Heterojunction on Photoelectrocatalytic Properties of ZnO−TiO_2 Films. *Int. J. Hydrogen Energy* **2007**, *32*, 3137−3140.
(21) Zhang, Z. H.; Yuan, Y.; Fang, Y. J.; Liang, L. H.; Ding, H. C.; Jin, L. T. Preparation of Photocatalytic Nano-ZnO/TiO_2 Film and Application for Determination of Chemical Oxygen Demand. *Talanta* **2007**, *73*, 523−528.
(22) Decher, G. Fuzzy Nanoassemblies: Toward Layered Polymeric Multicomposites. *Science* **1997**, *277*, 1232−1237.
(23) Kotov, N. A.; Dekany, I.; Fendler, J. H. Layer-by-Layer Self-Assembly of Polyelectrolyte-Semiconductor Nanoparticle Composite Films. *J. Phys. Chem.* **1995**, *99*, 13065−13069.
(24) Sakai, N.; Prasad, G. K.; Ebina, Y.; Takada, K.; Sasaki, T. Layer-by-Layer Assembled TiO_2 Nanoparticle/PEDOT-PSS Composite Films for Switching of Electric Conductivity in Response to Ultraviolet and Visible Light. *Chem. Mater.* **2006**, *18*, 3596−3598.
(25) Liu, Z. Y.; Zhang, X. T.; Nishimoto, S.; Jin, M.; Tryk, D. A.; Murakami, T.; Fujishima, A. Anatase TiO_2 Nanoparticles on Rutile TiO_2 Nanorods: A Heterogeneous Nanostructure via Layer-by-Layer Assembly. *Langmuir* **2007**, *23*, 10916−10919.
(26) He, J. A.; Mosurkal, R.; Samuelson, L. A.; Li, L.; Kumar, J. Dye-sensitized Solar Cell Fabricated by Electrostatic Layer-by-Layer Assembly of Amphoteric TiO_2 Nanoparticles. *Langmuir* **2003**, *19*, 2169−2174.
(27) Lee, D.; Rubner, M. F.; Cohen, R. E. All-Nanoparticle Thin-Film Coatings. *Nano Lett.* **2006**, *6*, 2305−2312.
(28) Lee, D.; Omolade, D.; Cohen, R. E.; Rubner, M. F. pH-Dependent Structure and Properties of TiO_2/SiO_2 Nanoparticle Multilayer Thin Films. *Chem. Mater.* **2007**, *19*, 1427−1433.
(29) DeRocher, J. P.; Mao, P.; Kim, J. Y.; Han, J.; Rubner, M. F.; Cohen, R. E. Layer-by-Layer Deposition of All-Nanoparticle Multilayers in Confined Geometries. *ACS Appl. Mater. Interfaces* **2012**, *4*, 391−396.
(30) Zhang, J. Y.; Feng, H. B.; Hao, W. C.; Wang, T. M. Luminescent Properties of ZnO Sol and Film Doped with Tb^{3+} Ion. *Mater. Sci. Eng., A* **2006**, *425*, 346−348.
(31) Kooli, F.; Chisem, I. C.; Vucelic, M.; Jones, W. Synthesis and Properties of Terephthalate and Benzoate Intercalates of Mg−Al Layered Double Hydroxides Possessing Varying Layer Charge. *Chem. Mater.* **1996**, *8*, 1969−1977.
(32) Anta, J. A.; Guillén, E.; Tena-Zaera, R. ZnO-Based Dye-Sensitized Solar Cells. *J. Phys. Chem. C* **2012**, *116*, 11413−11425.
(33) Kormann, C.; Bahnemann, D. W.; Hoffmann, M. R. Preparation and Characterization of Quantum-size Titanium Dioxide. *J. Phys. Chem.* **1988**, *92*, 5196−5201.
(34) Peiró, A. M.; Peral, J.; Domingo, C.; Domènech, X.; Ayllón, J. A. Low-Temperature Deposition of TiO_2 Thin Films with Photocatalytic Activity from Colloidal Anatase Aqueous Solutions. *Chem. Mater.* **2001**, *13*, 2567−2573.
(35) He, X. L.; Liu, M.; Yang, G. J.; Yao, H. L.; Fan, S. Q.; Li, C. J. Photovoltaic Performance Degradation and Recovery of the Flexible Dye-Sensitized Solar Cells by Bending and Relaxing. *J. Power Sources* **2013**, *226*, 173−178.
(36) Spanhel, L.; Anderson, M. A. Semiconductor Clusters in the Sol-Gel Process: Quantized Aggregation, Gelation, and Crystal Growth in Concentrated ZnO Colloids. *J. Am. Chem. Soc.* **1991**, *113*, 2826−2833.
(37) Hong, W. K.; Sohn, J. I.; Hwang, D. K.; Kwon, S. S.; Jo, G.; Song, S.; Kim, S. M.; Ko, H. J.; Park, S. J.; Welland, M. E.; Lee, T. Tunable Electronic Transport Characteristics of Surface-Architecture-Controlled ZnO Nanowire Field Effect Transistors. *Nano Lett.* **2008**, *8*, 950−956.
(38) Hayden, S. C.; Allam, N. K.; El-Sayed, M. A. TiO_2 Nanotube/CdS Hybrid Electrodes: Extraordinary Enhancement in the Inactivation of Escherichia coli. *J. Am. Chem. Soc.* **2010**, *132*, 14406−14408.
(39) Patrocínio, A. O. T.; Paterno, L. G.; Murakami Iha, N. Y. Layer-by-Layer TiO_2 Films as Efficient Blocking Layers in Dye-Sensitized Solar Cells. *J. Photochem. Photobiol., A* **2009**, *205*, 23−27.
(40) Zhi, Y.; Li, Y. G.; Zhang, Q. H.; Wang, H. Z. ZnO Nanoparticles Immobilized on Flaky Layered Double Hydroxides as Photocatalysts with Enhanced Adsorptivity for Removal of Acid Red G. *Langmuir* **2010**, *26*, 15546−15553.
(41) Yuan, S. J.; Mao, R. Y.; Li, Y. G.; Zhang, Q. H.; Wang, H. Z. Layer-by-Layer Assembling TiO_2 Film from Anatase TiO_2 Sols as the Photoelectrochemical Sensor for the Determination of Chemical Oxygen Demand. *Electrochim. Acta* **2012**, *60*, 347−353.
(42) Serpone, N.; Maruthamuthu, P.; Pichat, P.; Pelizzetti, E.; Hidaka, H. Exploiting the Interparticle Electron Transfer Process in the Photocatalysed Oxidation of Phenol, 2-Chlorophenol and Pentachlorophenol: Chemical Evidence for Electron and Hole Transfer Between Coupled Semiconductors. *J. Photochem. Photobiol., A* **1995**, *85*, 247−255.
(43) Zhang, W. D.; Jiang, L. C.; Ye, J. S. Photoelectrochemical Study on Charge Transfer Properties of ZnO Nanowires Promoted by Carbon Nanotubes. *J. Phys. Chem. C* **2009**, *113*, 16247−16253.
(44) Quintana, M.; Edvinsson, T.; Hagfeldt, A.; Boschloo, G. Comparison of Dye-Sensitized ZnO and TiO_2 Solar Cells: Studies of Charge Transport and Carrier Lifetime. *J. Phys. Chem. C* **2007**, *111*, 1035−1041.
(45) Talgorn, E.; de Vries, M. A.; Siebbeles, L. D. A.; Houtepen, A. J. Photoconductivity Enhancement in Multilayers of CdSe and CdTe Quantum Dots. *ACS Nano* **2011**, *5*, 3552−3558.